

Orientation dependence in high harmonics of ZnO with polarization corrections to counteract the birefringent effect

Yin-Fu Zhang(张银福), Teng-Fei Huang(黄腾飞), Jia-Peng Li(李佳鹏), Ke Yang(杨可), Liang Li(李亮), Xiao-Song Zhu(祝晓松), Peng-Fei Lan(兰鹏飞), and Pei-Xiang Lu(陆培祥)

Citation: Chin. Phys. B, 2021, 30 (**7**): 074204. DOI: 10.1088/1674-1056/abf3b9
Journal homepage: http://cpb.iphy.ac.cn; http://iopscience.iop.org/cpb

What follows is a list of articles you may be interested in

Quantum plasmon enhanced nonlinear wave mixing in graphene nanoflakes

Hanying Deng(邓寒英), Changming Huang(黄长明), Yingji He(何影记), and Fangwei Ye(叶芳伟)
Chin. Phys. B, 2021, 30 (**4**): 044213. DOI: 10.1088/1674-1056/abea8d

High-efficiency terahertz wave generation with multiple frequencies by optimized cascaded difference frequency generation

Zhongyang Li(李忠洋), Binzhe Jiao(焦彬哲), Wenkai Liu(刘文锴), Qingfeng Hu(胡青峰), Gege Zhang(张格格), Qianze Yan(颜钤泽), Pibin Bing(邴丕彬), Fengrui Zhang(张风蕊), Zhan Wang(王湛), and Jianquan Yao(姚建铨)
Chin. Phys. B, 2021, 30 (**4**): 044211. DOI: 10.1088/1674-1056/abe3eb

Theoretical research on terahertz wave generation from planar waveguide by optimized cascaded difference frequency generation

Zhongyang Li(李忠洋), Jia Zhao(赵佳), Wenkai Liu(刘文锴), Qingfeng Hu(胡青峰), Yongjun Li(李永军), Binzhe Jiao(焦彬哲), Pibin Bing(邴丕彬), Hongtao Zhang(张红涛), Lian Tan(谭联), and Jianquan Yao(姚建铨)
Chin. Phys. B, 2021, 30 (**2**): 024209. DOI: 10.1088/1674-1056/abc3b7

Spectral redshift of high-order harmonics by adding a weak pulse in the falling part of the trapezoidal laser pulse

Xue-Fei Pan(潘雪飞), Jun Zhang(张军), Shuai Ben(贲帅), Tong-Tong Xu(徐彤彤), Xue-Shen Liu(刘学深)
Chin. Phys. B, 2018, 27 (**2**): 024206. DOI: 10.1088/1674-1056/27/2/024206

Generation of isolated attosecond pulses in bowtie-shaped nanostructure with three-color spatially inhomogeneous fields

Xue Shan, Du Hong-Chuan, Xia Yue, Hu Bi-Tao
Chin. Phys. B, 2015, 24 (**5**): 054210. DOI: 10.1088/1674-1056/24/5/054210

Orientation dependence in high harmonics of ZnO with polarization corrections to counteract the birefringent effect*

Yin-Fu Zhang(张银福)[1], Teng-Fei Huang(黄腾飞)[1], Jia-Peng Li(李佳鹏)[1], Ke Yang(杨可)[1], Liang Li(李亮)[1,†], Xiao-Song Zhu(祝晓松)[1], Peng-Fei Lan(兰鹏飞)[1,‡], and Pei-Xiang Lu(陆培祥)[1,2,3]

[1] *School of Physics and Wuhan National Laboratory for Optoelectronics, Huazhong University of Science and Technology, Wuhan* 430074, *China*

[2] *Hubei Key Laboratory of Optical Information and Pattern Recognition, Wuhan Institute of Technology, Wuhan* 430205, *China*

[3] *CAS Center for Excellence in Ultraintense Laser Science, Shanghai* 201800, *China*

(Received 11 January 2021; revised manuscript received 23 March 2021; accepted manuscript online 31 March 2021)

We investigate the influence of the birefringence on the high-order harmonics in an a-cut ZnO crystal with mid-infrared laser pulses. The high harmonics exhibit strong dependence on the alignment of the crystal with respect to the laser polarization. We introduce the Jones calculus to counteract the birefringent effect and obtain the harmonics with polarization corrections in ZnO. We show that the birefringent effect plays an important role in the orientation dependence of HHG.

Keywords: high-order harmonics, birefringent effect, Jones calculus

PACS: 42.65.Ky, 42.25.Lc, 02.10.Yn **DOI:** 10.1088/1674-1056/abf3b9

1. Introduction

High-order harmonic generation (HHG) in gaseous media has led to significant advances in the study of molecular electron dynamics on the attosecond time scales.[1–10] Because the information of the target structure is encoded in the HHG, a technology called molecular orbital tomography has been developed.[11–14] Recently, the developments of HHG in the solids have opened a new frontier in the ultrafast science. Since Ghimire *et al.* observed HHG in the ZnO crystal using mid-infrared (mid-IR) laser pulses,[15] harmonics generated from various crystals have been reported.[16–24] Similar to the HHG in the gases, the solid structures are related to the dependence of harmonic yields on the orientation of the crystal axis. Different from the gas-phase media, solids have periodic structures and can be precisely aligned to a certain orientation. It is expected to have great potential for band-structure reconstruction[25–28] and probing electron dynamics[29,30] by using the HHG in solids. Whereas, the harmonics in solids are coupled with the propagation effect, such as the absorption, phase mismatch of HHG,[31] and the birefringence of the crystals. It may affect the HHG in solids. However, the effect of birefrigence is not explored in previous works of HHG in ZnO.[20,32,33]

In the past several years, the propagation effect has been studied in some crystals.[31,34–37] In Ref. [36], Vampa *et al.* investigated the HHG in a reflection geometry with MgO and Si. They predicted the variation of the high-harmonic power with the angle of incidence by introducing the nonlinear reflection coefficients. By using both the reflection and transmission geometries, Xia *et al.* studied the propagation effect in the HHG of GaAs.[37] They observed that the orientation dependence of HHG in the transmission geometry becomes more anisotropic for the thicker sample. In contrast, the orientation dependence of HHG in the reflection geometry is less anisotropic than that in the transmission geometry. When the laser pulses propagate through the crystal, the polarization can be altered from linear to elliptical because of the birefringent effect. Whereas, the influence of the change on the HHG in solids has not been discussed clearly.

In this paper, we measure the harmonics in a ZnO crystal as a function of the alignment of the optic axis with respect to the laser polarization. The orientation dependence of the HHG spectra is affected by the birefringence of ZnO. We find that the birefringent effect can be described by a Jones matrix even in the intense field. We introduce the Jones calculus to correct the laser polarization. We obtain the orientation-dependent harmonics with linear polarized laser pulses at the last layers of the ZnO crystal. There are distinctions between the harmonics with polarization corrections and the signals without the corrections.

2. Experimental setup

In our experiment, we use a transmission geometry. The sample is a 500-μm-thick a-cut ZnO crystal. Its roughness is less than 5 Å, and the purity is more than 99.99%. The transmission spectra and x-ray diffraction data refer to

*Project supported by the National Natural Science Foundation of China (Grant Nos. 91950202, 11627809, 11874165, 11934006, 11774109, and 12021004).

†Corresponding author. E-mail: liangl@hust.edu.cn

‡Corresponding author. E-mail: pengfeilan@hust.edu.cn

© 2021 Chinese Physical Society and IOP Publishing Ltd

Refs. [38,39]. The mid-IR pulse (center wavelength of 2.4 μm, temporal duration of 150 fs) is produced by a commercial optical parametric amplifier (OPA, Light Conversion TOPAS-prime) pumped by an amplified Ti:sapphire laser system (Legend Elite Duo, Coherent, Inc.). The repetition rate is 1 kHz.

The laser pulse is focused into the crystal at a normal incidence with a lens of 50-mm focal length. The spot size is about 150 μm in vacuum, which is measured by a knife-edge scan. To control the alignment with respect to the laser polarization and the field strength, we mount the crystal to allow rotation about its normal and translation through the laser focus. We use a half-wave plate (HWP) and a quarter-wave plate (QWP), which are set in front of the focusing lens, to control the polarization of the incident laser pulse. At the exit of the crystal, we use a combination of a polarizer (WP25M-UB, Thorlabs) and a power meter to analyse the polarization of the emitted laser pulse. HHG signals are collimated by a 50-mm-focal-length lens and focused by a lens with the same focal length. Then the signals are collected to a spectrometer with a 150 g·mm^{-1} grating and detected by an intensified charge-coupled device camera (ICCD, PI-MAX1024UV).

3. Results and discussion

The schematic of the ZnO crystal is shown in Fig. 1(a). The blue shaded region shows the a-cut plane. The laser polarization, shown as a black arrow, is lying in this plane. θ indicates the angle between the optic axis and the laser polarization. As shown in Fig. 1(b), the measured spectrum covers harmonics from 4th to 9th order. The conversion efficiency of harmonics is estimated to be from 2.5×10^{-5} (4th) to 1.0×10^{-7} (9th). The HHG spectra are measured as a function of θ. The wavelength of the laser field is centered at 2.4 μm and the strength is about 0.9 TW/cm^2. Under this field strength, we observe the maximum yield of HHG without optical damage. The even harmonics are at their maxima when the laser polarization is along 0° or 180°, which correspond to the optic axis. And they are at their minima when the laser polarization is along 90°. The periodicity of even harmonics is π. In addition, secondary peaks appear near 60° and 120° for the even harmonics. The odd harmonics show their maxima when the laser polarization is along 0°, 90°, and 180°. The periodicity of odd harmonics is $\pi/2$.

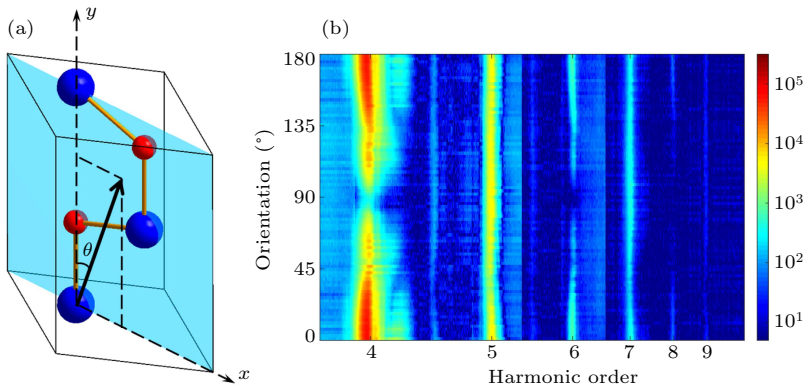


Fig. 1. (a) Schematic of the wurtzite ZnO crystal with shaded region showing an a-cut plane. The Zn is shown in blue and slightly larger than the red O. The laser polarization is shown as the black arrow, and the angle θ, between the optic axis and the laser polarization is indicated. (b) High-order harmonic spectra as a function of the crystallographic orientation with respect to the polarization of the laser pulse. The crystal is rotated about the laser propagation axis to vary the angle between the laser polarization and the optic axis. The field is centered at 2.4 μm, and the strength is about 0.9 TW/cm^2. The intensity of harmonics is normalized in arb. units. The periodicity of odd harmonics is $\pi/2$, and the periodicity of even harmonics is π.

To eliminate the birefringent effect, we need to quantify the variation of the laser polarization. Because of the absorption of the harmonics above the bandgap (3.2 eV), the generation of high order harmonics is limited to the last few tens of nanometres of ZnO.[15] Therefore we measure the polarization of the transmitted laser pulse to quantify the variation of the polarization. We obtain the polarization state of the emitted laser pulse by using the analysis system, which contains a polarizer and a power meter (see Section 2). The results are shown as red solid lines in Fig. 2. We can observe that the laser pulse remains linear when it is parallel (0°) or perpendicular (90°, not shown in the figure) to the optic axis of the crystal. When the crystal is rotated along different orientations, the ellipticity of the pulses changes from 0.05 (0°) to 0.37 (45°). Unless otherwise indicated, the ellipticity is defined as $\sqrt{I_{\min}/I_{\max}}$, where $I_{\min}$ ($I_{\max}$) is the minimum (maximum) transmitted intensity of the polarimetry scan by rotating the polarizer. The laser polarization changes from elliptical to linear when the rotation angle increases from 45° to 90°. To quantify the birefringent effect of ZnO, we use the Jones calculus to describe the birefringent effect in the ZnO crystal.

The incident laser pulse is expressed as

$$\boldsymbol{J}_{\text{incident}} = \begin{bmatrix} E\sin\theta \\ E\cos\theta \end{bmatrix}, \tag{1}$$

where E is the electric field of the incident laser pulse. Then we model the birefringent effect of ZnO crystal as a matrix, $\boldsymbol{R}$. From Fig. 2, we observe that the orientation of the major axis

of the transmitted laser pulse is the same as that of the incident pulse. Only the ellipticity changes. So the Jones matrix can be given by

$$\boldsymbol{R} = \begin{bmatrix} 1 & 0 \\ 0 & k \cdot \mathrm{e}^{\mathrm{i}\varphi} \end{bmatrix}, \tag{2}$$

where k is the coefficient of the amplitude of the electric field, and φ is the phase difference between x-component and y-component of the electric field. The transmitted pulse after propagation in the crystal is given as following:

$$\boldsymbol{J}_{\text{emitted}} = \boldsymbol{R} \cdot \boldsymbol{J}_{\text{incident}}. \tag{3}$$

By fitting the value of $\boldsymbol{J}_{\text{emitted}}$ to the experiment, we get the value of $\boldsymbol{R}$, which is given by

$$\boldsymbol{R} = \begin{bmatrix} 1 & 0 \\ 0 & 1.0571 \cdot \mathrm{e}^{0.7172\mathrm{i}} \end{bmatrix}. \tag{4}$$

The fitting results are shown as the blue dash lines in Fig. 2. They are in good agreement with the experimental data (shown as the red solid lines in Fig. 2). The agreement confirms that it is reasonable to use the Jones matrix to describe the birefringent effect of ZnO crystal even in the intense laser field.

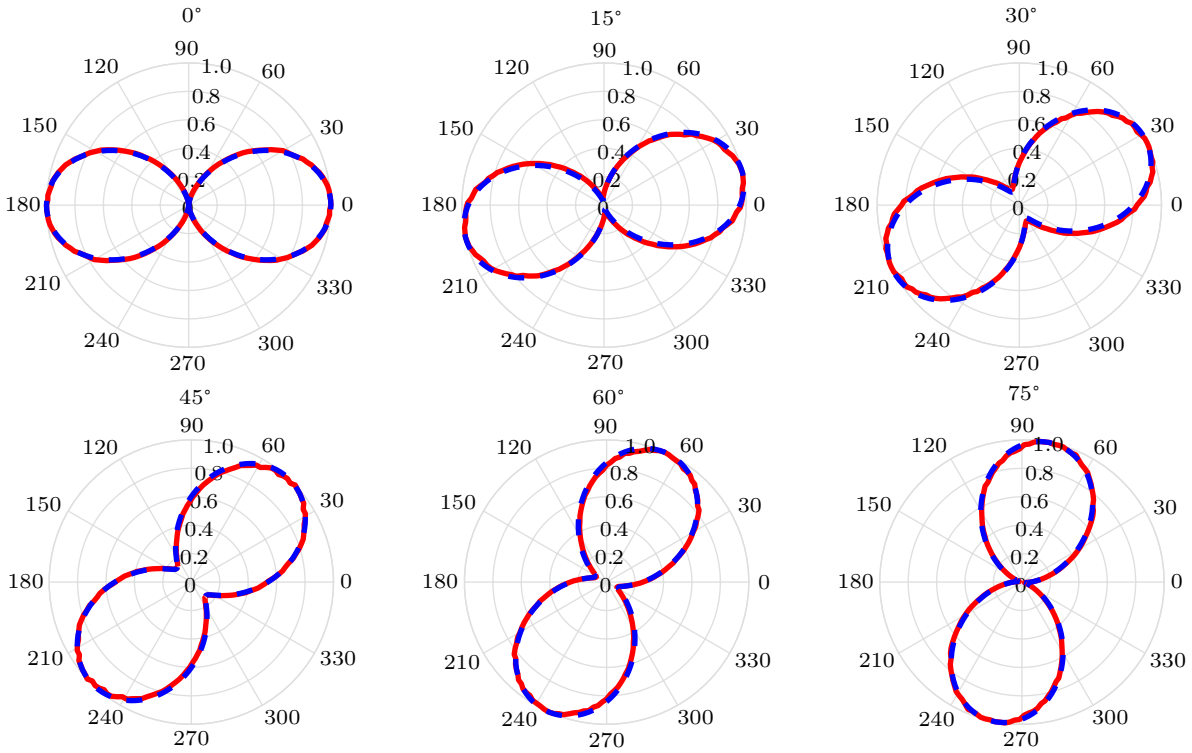


Fig. 2. Polarization of the laser pulse after passing through the ZnO crystal in the experiment (red solid lines) and the Jones calculus calculations (blue dash lines). The title is the angle between the polarization of the incident laser with the optic axis of the crystal. The intensity is normalized by the maximum. The ellipticity of the emitted laser changes from 0.05 (linear, 0° or 90°) to 0.38 (elliptical, 45°).

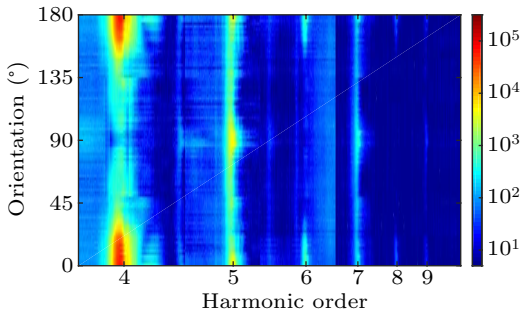


Fig. 3. High-order harmonic spectra as a function of the alignment of the crystal with respect to the polarization of the laser pulse by counteracting the birefringent effect. The wavelength and field strength of the laser pulse are same as those in Fig. 1. The periodicity of odd harmonics and even harmonics is $\pi/2$ and π, respectively.

Then we use the inverse matrix, $\boldsymbol{R}^{-1}$, to counteract the birefringent effect. We firstly calculate the polarization of the incident laser pulse by $\boldsymbol{J}_{\text{incident}} = \boldsymbol{R}^{-1} \cdot \boldsymbol{J}_{\text{emitted}}$. By controlling the angles of the HWP and QWP in front of the focusing lens, we alter the polarization of the incident laser to make sure that the transmitted laser is linearly polarized along a specific direction. Then we measure the orientation dependence of the HHG using the corrected polarization laser pulses. The measurement results are shown in Fig. 3. The wavelength and the field strength of the laser pulse are the same as those in Fig. 1. One can clearly see some distinctions compared with the HHG spectra in Fig. 1.

To show the distinction clearly, we compare the HHG with polarization corrections to the signal without corrections in Fig. 4. The blue dots are the HHG signal with the birefringent effect, and the red dots are the HHG with polarization corrections. By comparing to the even harmonics without polarization corrections, the modulation of the even harmonics from 45° to 135° is much smaller after the polarization correction. Moreover, the secondary peaks of even harmonics disappear after the polarization correction. It shows that

the secondary peaks originate from the change of the laser polarization. For the odd harmonics, the intensity with polarization corrections exhibits a deeper modulation compared to that without polarization correction. The ratio between the minimum and the maximum of the 5th-order harmonic is about 0.32 (0.38 for the 7th-order harmonic, 0.5 for the 9th-order harmonic) without polarization correction. The ratio becomes about 0.1 for the 5-th order harmonics (0.15 for the 7th-order harmonic, 0.25 for the 9th-order harmonic) with polarization correction. Furthermore, the birefringence affects the symmetry of the HHG signal. As shown in Fig. 4, the symmetry axis is at 90°. The symmetry of the HHG with polarization corrections is excellent. But for the HHG without the corrections, the intensity along θ (from 0° to 90°) is smaller than that along $180° - \theta$. These comparisons show that the secondary peaks, the small modulation, and the asymmetry of the HHG are associated with the birefringent effect. Some extra features are coupled in the orientation dependence of the HHG without polarization correction. It will affect the understanding of the generation mechanism of the HHG. Moreover, we need to eliminate the birefringent effect to obtain the original signals and retrieve the solid structure.

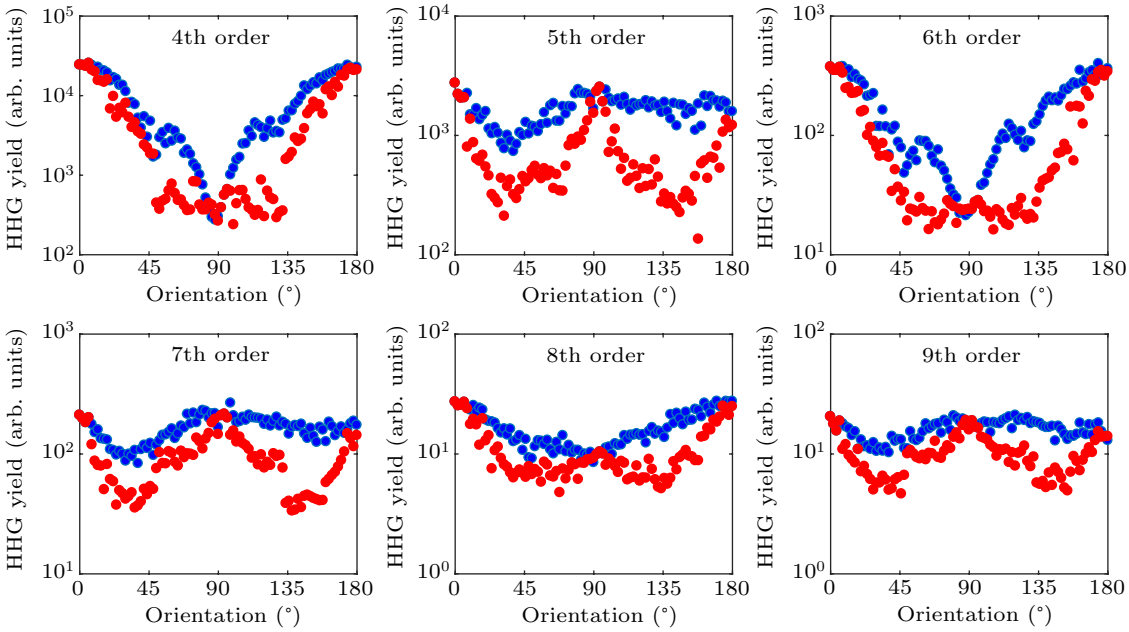


Fig. 4. Comparison of the HHG spectra from transmission through the bulk ZnO and that with polarization corrections by using the Jones calculus. The blue dots are the measurements with the birefringent effect, and the red dots are the HHG spectra counteracting the effect by using the Jones calculus.

4. Conclusion

We report the HHG spectra in ZnO as a function of the alignment angle between the laser polarization and the optic axis. The harmonics are affected by the birefringent effect of the crystal. By introducing the Jones calculus, we counteract the birefringent effect and obtain the HHG spectra with polarization corrections. There is explicit distinction in the HHG spectra compared with the uncorrected signals. Without the birefringent effect, the modulation of the odd harmonics is deeper and the even harmonics have no secondary peaks. It is important to eliminate the birefringent effect from the HHG to reflect the original structure of solid.

References

[1] Hentschel M, Kienberger R, Spielmann C, Reider G, Milosevic N, Brabec T, Corkum P, Heinzmann U, Drescher M and Krausz F 2001 *Nature* **414** 509

[2] He L X, Zhang Q B, Lan P F, Cao W, Zhu X S, Zhai C Y, Wang F, Shi W J, Li M, Bian X B, Lu P X and Bandrauk A D 2018 *Nat. Commun.* **9** 1108

[3] Paul P M, Toma E S, Breger P, Mullot G, Auge F, Balcou P, Muller H G and Agostini P 2001 *Science* **292** 1689

[4] Corkum P B and Krausz F 2007 *Nat. Phys.* **3** 381

[5] He Y Q, He L X, Wang P, Wang B C, Sun S Q, Liu R X, Wang B N, Lan P F and Lu P X 2020 *Opt. Express* **28** 21182-21191

[6] Niikura H, Legare F, Hasbani R, Bandrauk A D, Ivanov M, Villeneuve D M and Corkum P B 2002 *Nature* **417** 917

[7] Shao R Z, Zhai C Y, Zhang Y F, Sun N, Cao W, Lan P F and Lu P X 2020 *Opt. Express* **28** 15874

[8] Kanai T, Minemoto S and Sakai H 2005 *Nature* **435** 470

[9] Li W, Zhou X, Lock R, Patchkovskii S, Stolow A, Kapteyn H C and Murnane M M 2008 *Science* **322** 1207

[10] Sun N, Zhu X S, Wang B C, Wang D, Shao R Z, Lan P F and Lu P X 2020 *Phys. Rev. A* **101** 053437

[11] Itatani J, Levesque J, Zeidler D, Niikura H, Pepin H, Kieffer J C, Corkum P B and Villeneuve D M 2004 *Nature* **432** 867

[12] Zhai C Y, Zhang X F, Zhu X S, He L X, Zhang Y F, Wang B N, Zhang Q B, Lan P F and Lu P X 2018 *Opt. Express* **26** 2775

[13] Haessler S, Caillat J and Salieres P 2011 *J. Phys. B: At. Mol. Opt. Phys.* **44** 203001

[14] Wang B C, He Y Q, Zhao X F, He L X, Lan P F, Lu P X and Lin C D 2020 *Phys. Rev. A* **101** 063417

[15] Ghimire S, DiChiara A D, Sistrunk E, Agostini P, DiMauro L F and Reis D A 2011 *Nat. Phys.* **7** 138

[16] Schubert O, Hohenleutner M, Langer F, Urbanek B, Lange C, Huttner U, Golde D, Meier T, Kira M, Koch S W and Huber R 2014 *Nat. Photon.* **8** 119

[17] Luu T T, Garg M, Kruchinin S Y, Moulet A, Hassan M T and Goulielmakis E 2015 *Nature* **521** 7553
[18] Liu H, Li Y, You Y S, Ghimire S, Feinz T F and Reis D A 2016 *Nat. Phys.* **13** 262
[19] Sivis M, Taucer M, Vampa G, Johnston K, Staudte A, Naumov A Y, Villeneuve D M, Ropers C and Corkum P B 2017 *Science* **357** 303
[20] Gholam-Mirzaei S, Beetar J and Chini M 2017 *Appl. Phys. Lett.* **110** 061101
[21] Huang T F, Zhu X S, Li L, Liu X, Lan P F and Lu P X 2017 *Phys. Rev. A* **96** 043425
[22] You Y S, Reis D A and Ghimire S 2017 *Nat. Phys.* **13** 345
[23] Yoshikawa N, Tamaya T and Tanaka K 2017 *Science* **356** 6339
[24] Li J P, Zhang Q B, Li L, Zhu X S, Huang T F, Lan P F and Lu P X 2019 *Phys. Rev. A* **99** 033421
[25] Vampa G, Hammond T J, Thire N, Schmidt B E, Legare F, McDonald C R, Brabec T, Klug D D and Corkum P B 2015 *Phys. Rev. Lett.* **115** 193603
[26] Lanin A A, Stepanov E A, Fedotov A B and Zheltikov A M 2017 *Optica* **4** 5
[27] Li L, Lan P F, He L X, Cao W, Zhang Q B and Lu P X 2020 *Phys. Rev. Lett.* **124** 157403
[28] Yu C, Jiang S, Wu T, Yuan G, Wang Z, Jin C and Lu R 2018 *Phys. Rev. B* **98** 085439
[29] Schultze M, Ramasesha K, Pemmaraju C D, Sato S A, Whitmore D, Gandman A, Prell J S, Borja L J, Prendergast D, Yabana K, Neumark D M and Leone S R 2014 *Science* **346** 1348
[30] Garg M, Zhan M, Luu T T, Lakhotia H, Klostermann T, Guggenmos A and Goulielmakis E 2016 *Nature* **538** 7625
[31] Ghimire S, DiChiara A D, Sistrunk E, Ndabashimiye G, Szafruga U B, Mohammad A, Agostini P, DiMauro L F and Reis D A 2012 *Phys. Rev. A* **85** 043836
[32] Jiang S C, Mirzaei S G, Crites E, Beetar J E, Singh M, Lu R F, Chini M and Lin C D 2019 *J. Phys. B: At. Mol. Opt. Phys.* **52** 225601
[33] Liu C D, Zheng Y H, Zeng Z N and Li R X 2016 *Phys. Rev. A* **93** 043806
[34] Crites Erin L 2020 *Polarization dependence of high order harmonic generation from solids in reflection and transmission geometries* (Honors Undergraduate Theses) 693
[35] Vampa G, Liu H, Heinz T F and Reis D A 2018 *Conference on Lasers and Electro-Optics*, May 13–18, 2018, San Jose, CA, USA, pp. 1–2
[36] Vampa G, You Y S, Liu H, Ghimire S and Reis D A 2018 *Opt. Express* **26** 12210
[37] Xia P, Kim C, Lu F, Kanai T, Akiyama H, Itatani J and Ishii N 2018 *Opt. Express* **26** 22
[38] Ratheesh Kumar P M, Kartha C S and Vijayakumar K P 2005 *J. Appl. Phys.* **97** 013509
[39] Wan B Y 2007 *Laser Journal* **28** 6